J|A|C|S COMMUNICATIONS

Published on Web 11/02/2009

Nonpolymeric Thermosensitive Supramolecules

José E. Betancourt and José M. Rivera*

Department of Chemistry, University of Puerto Rico, Río Piedras Campus, Río Piedras, Puerto Rico 00931

Received August 21, 2009; E-mail: jmrivortz@mac.com

Naturally occurring molecular machines self-assemble into a wide variety of nanostructures that are able to sense environmental changes and respond to them accordingly. Artificial stimuli responsive (i.e., smart) materials have found numerous applications in biomedicine and nanotechnology.[1] This is due to their ability to undergo large changes in a property triggered by a relatively small stimulus. In thermosensitive materials, when a water-soluble substance is made increasingly hydrophobic, it will reach a range of compositions upon which it will show a lower critical solution temperature (LCST) before becoming completely insoluble.[2] Polymers represent the overwhelming majority of known substances that show the LCST phenomenon by undergoing a coil to globule transition and/or self-assembling into aggregates upon reaching a transition temperature (T_t).[1c,3,4] Thermally responsive polymers, most notably, elastin-like polypeptides (ELPs)[5] and poly(*N*-isopropylacrylamide) (pNIPAAm),[6] are attractive due to their suitability for fundamental studies as well as their practical uses in a plethora of applications.[7−11]

Although, in principle, nonpolymeric and well-defined supramolecular assemblies could be developed to show this property, to the best of our knowledge, there are still no known examples of such substances. Here we show 2′-deoxyguanosine derivatives that self-assemble in aqueous media into discrete supramolecular hexadecamers and exhibit the LCST phenomenon. Furthermore, the T_t can be tuned to higher values by the addition of a more hydrophilic derivative. These findings uncover a new paradigm in the development of smart thermosensitive materials with properties and applications complementary to those of polymers.[4]

Supramolecular self-assembly offers a complementary biomimetic strategy to the use of polymers for the development of functional nanostructures.[1,12,13] Attractive features of supramolecular self-assembly include synthetic economy and the dynamic exchange of subunits. Our efforts in this field have been aimed at studying the self-assembly of 2′-deoxyguanosine derivatives, in particular, modulation of the resulting supramolecular structures by replacing H8 in the guanine moiety with a functionalized aryl group (Figure 1).[14] We have shown that the nature and substitution pattern of the aryl group can dictate the molecularity and stability (thermal and kinetic) of the resulting supramolecules as well as their selectivity for binding metal cations.[14c] Furthermore, we have shown the reversible high fidelity switching between a hexadecamer and an octamer by simply changing the solvent.[14d]

The 8-(*meta*-acetylphenyl)-2′-deoxyguanosine (mAG) moiety is an attractive recognition motif that enables the construction of well-defined and discrete supramolecular nanostructures.[15] We demonstrated this by using it to construct lipophilic hexadecameric self-assembled dendrimers (SADs).[16] Our recent discovery that a positively charged hydrophilic mAG derivative self-assembles isostructurally into hexadecamers in aqueous media[15] prompted us to explore the construction of hydrophilic SADs. During such studies, we discovered that, upon assembly, derivative **2** (Figure 1a) exhibited the LCST phenomenon (*vide infra*).

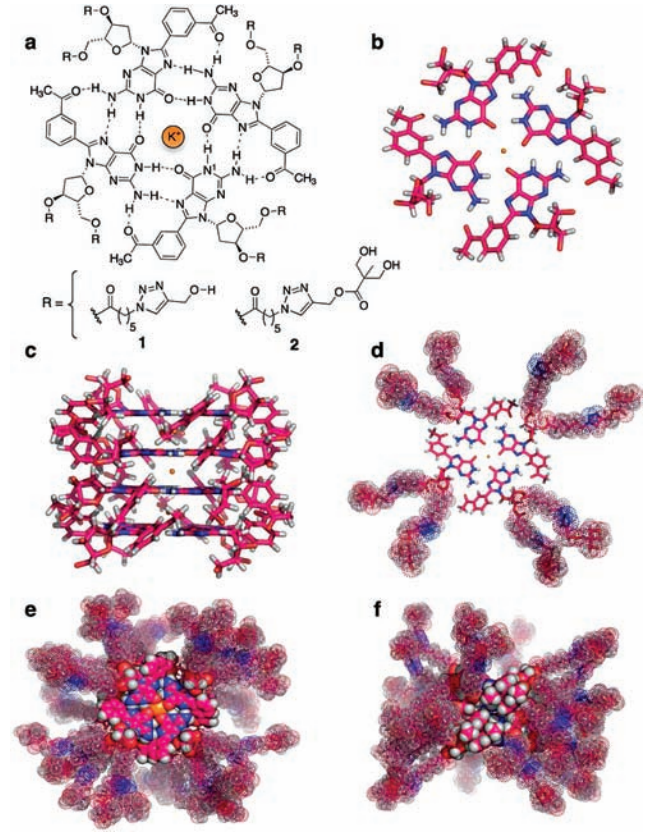

Figure 1. (a) Chemical structure of the tetrad formed by **1** and **2**. (b) Top view of the tetrad shown in a. (c) Side view of the hexadecamer $\mathbf{2}_{16}$•3KI (abbreviated throughout the article as $\mathbf{2}_{16}$), formed by four coaxially stacked tetrads. In b and c the ester side chains attached to the 2′-deoxyribose rings are omitted for clarity. (d) Same as b but with the ester groups highlighted with a dotted surface. (e) Similar to d in CPK representation and with the ester groups of all the subunits shown. (f) Side view of e. In all the models the carbon atoms are magenta, the oxygen atoms are red, the nitrogen atoms are blue, the potassium cations are yellow, and the hydrogen atoms are white.

Both **1** and **2** (Figure 1a,b) were synthesized using a methodology similar to that previously reported by us[16] (Figure S1).[17] At room temperature, both derivatives are insoluble in an aqueous phosphate-buffered solution (pH 7.1), but upon addition of KI (2 M), they become soluble. ^{1}H NMR experiments of soluble solutions of **1** and **2** (both at 20 mM, pH 7.1, 2 M KI) in H_2O-D_2O (9:1, potassium buffer) reveal the signatures for the self-assembly in aqueous media. The ^{1}H NMR spectrum shows the characteristic double set of signals corresponding to two pairs of tetrads (N^1H) in different chemical environments (Figure 2a,b). The 2D NOESY spectrum supports the formation of $\mathbf{1}_{16}$ and $\mathbf{2}_{16}$, by showing the signature cross peaks characteristic of a hexadecamer in water[15] (Figure S7).[17] The enhanced solubility is not a simple salting-in process, but it also results from the self-assembly of 16 subunits in

10.1021/ja9070927 CCC: $40.75

which the more hydrophobic aryl components are clustered together in a central, relatively hydrophobic, core (Figure 1c), surrounded by the more hydrophilic groups (e.g., triazole rings, hydroxyl groups) facing the solvent (Figure 1d−f).

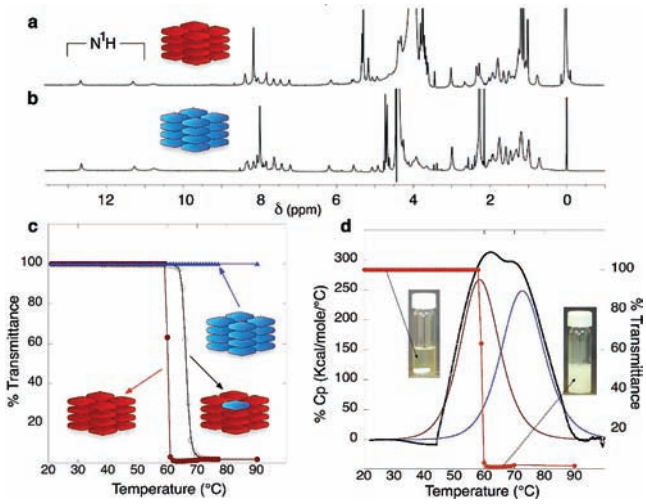

Figure 2. ^{1}H NMR spectra (500 MHz, 10% D_2O in H_2O), DSC, and turbidity data. (a) NMR spectrum of $\mathbf{2}_{16}$. (b) NMR spectrum of $\mathbf{1}_{16}$. The red and blue cartoons in a and b represent $\mathbf{2}_{16}$ and $\mathbf{1}_{16}$, respectively. (c) Turbidity curves (measured at 500 nm) for $\mathbf{2}_{16}$ (red circles), $\mathbf{1}_{16}$ (blue triangles), and the mixed $\mathbf{1}\bullet\mathbf{2}_{15}$ (hollow circles). The measurements were performed in aqueous phosphate-buffered solution (pH 7.1, 2 M KI). (d) DSC endotherm with the two resulting deconvolution peaks representing the T_t, left, and the T_m, right. The overlaid turbidity curve (red circle) shows an excellent correlation with the DSC peak that corresponds to the T_t. Insets, vials with a solution of $\mathbf{2}_{16}$ below, left, and above, right, the T_t.

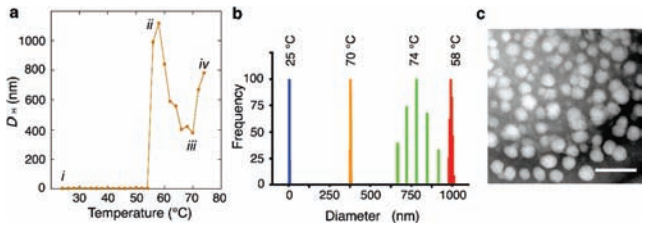

Figure 3. (a) Average hydrodynamic diameters (D_H) of $\mathbf{2}_{16}$ (orange squares) as a function of temperature measured by DLS. The measurements were made at intervals of 2 °C, allowing the temperature to stabilize before each measurement. (b) Size distributions for selected temperatures from the DLS curve shown on a (*i*−*iv*). (c) TEM image of a sample of $\mathbf{2}_{16}$ deposited above the T_t (60 °C). Scale bar, 200 nm. The apparent discrepancy between the D_H determined by DLS and TEM is likely due to the dehydration of the globules upon drying the sample and the high vacuum conditions of the TEM measurements.

The supramolecular state also leads to the emergence of the thermosensitive property for $\mathbf{2}_{16}$. Aqueous phosphate-buffered solutions (pH 7.1, 2 M KI) of both $\mathbf{1}_{16}$ and $\mathbf{2}_{16}$ were completely homogeneous (i.e., highly soluble) at room temperature. And while the turbidity for the solution of $\mathbf{1}_{16}$ does not change upon heating to 90 °C (Figure 2c, blue curve), the solution of $\mathbf{2}_{16}$ suddenly becomes cloudy at 59 °C. Transmittance measurements at 500 nm confirm these observations (Figure 2c, red curve). Cooling the solution back to 25 °C restores the initial conditions (yellowish transparent solution), and this process can be repeated at least ten times (Figure S9)[17] with no signs of fatigue (e.g., decomposition).

Differential scanning calorimetry (DSC) studies support the results obtained from the transmittance measurements and provide further insights into the energetics of the LCST phenomenon.[18] DSC measurements reveal a double-peak endotherm transition, which upon deconvolution reveal the overlap of two different processes with temperatures of 58.7 and 72.7 °C. The excellent overlap of the first peak with the transmittance curve indicates a direct correlation to the T_t. The close match between the endothermic DSC peak corresponding to the melting temperature of $\mathbf{1}_{16}$ (T_m = 77.2 °C, Figure S12)[17] and the second peak from the sample of $\mathbf{2}_{16}$ strongly suggests that it belongs to the melting of the hexadecamers within the suspended particles. The results from VT NMR experiments with $\mathbf{2}_{16}$ (T_m = 76.7 °C, Figure S11)[17] correlate well with those from the DSC. Furthermore, the signature peaks for the hexadecamer are observed at temperatures above the T_t, which is a strong indication that the hexadecamers undergo the phase transition intact (i.e., as well-defined supramolecules). This discards the possibility that the phase transition occurs because of a temperature induced disassembly followed by the precipitation of the monomeric subunits.

Modulating the T_t for any system that exhibits the LCST phenomenon can be achieved by adjusting the balance between hydrophobic and hydrophilic groups.[5,8,19] In polymeric systems, T_t is usually modulated by changing the composition at the synthesis level, but multiple other strategies such as changes in pH, ionic strength, and the presence of cosolutes, among others, are usually employed.[20] Simple blending procedures[21] and supramolecular modification of polymeric systems have also been used to achieve such modulation.[3a,22] This led us to hypothesize that adding the more hydrophilic **1** to a solution of $\mathbf{2}_{16}$ would lead to an increase in the T_t. A solution containing **1** to **2** (1:15, 20 mM combined) shows a ^{1}H NMR indicative of a fully mixed hexadecamer (Figure S8).[17] The T_t of this solution is 64.9 °C as determined by transmittance experiments (Figure 2c) and confirmed by DSC (Figure S13). Similar experiments using a greater proportion of **1** to **2** (1:1) also show the formation of a mixed hexadecamer, but this time no T_t was observed in the temperature range 25−90 °C (data not shown). At this point the system has overcome the threshold of the hydrophilic/hydrophobic balance required to show the LCST phenomenon.

Dynamic light scattering (DLS) studies provide critical information regarding the sizes of the various supramolecules as a function of temperature (24−74 °C). Below the T_t the average hydrodynamic diameter (D_H) for $\mathbf{2}_{16}$ is (4.6 ± 0.2) nm (Figure 3a), which is in very good agreement to the value obtained from ^{1}H DOSY NMR experiments of (4.40 ± 0.12) nm (Table S1).[17,23] Upon reaching T_t, the D_H of the sizes of the species in solution increased by 3 orders of magnitude to above 1 μm. Continued heating of the solution from 58.0 to 66.0 °C lead to a sharp decrease of the D_H until the values stabilized at ∼400 nm. Transmission electron microscopy (TEM) measurements of these aggregates showed that they are nonhollow, discrete, and globular nanoparticles of relatively low polydispersity (Figure 3c). Heating the sample beyond 70 °C leads to a sudden increase in the D_H values with a concomitant increase in the polydispersity of the resulting aggregates (Figure 3b, 74 °C).

Furthermore, the DLS studies allow us to postulate a mechanism for this thermally induced assembly (Figure 4). At 25−58 °C the solution is populated with monodisperse, discrete self-assembled hexadecamers (Figure 4b,*i*). Raising the temperature above the T_t (58 °C) induces the formation of large hydrated globules of intermediate polydispersity (Figure 4b,*ii*). A continued heating of the sample (60.0−70.0 °C) leads to a decrease in the average size of the globules (Figure 4b,*iii*). This is likely due to the ejection of water molecules initially trapped throughout the interior of the aggregates. Further heating of the solution (>70.0 °C) induces a

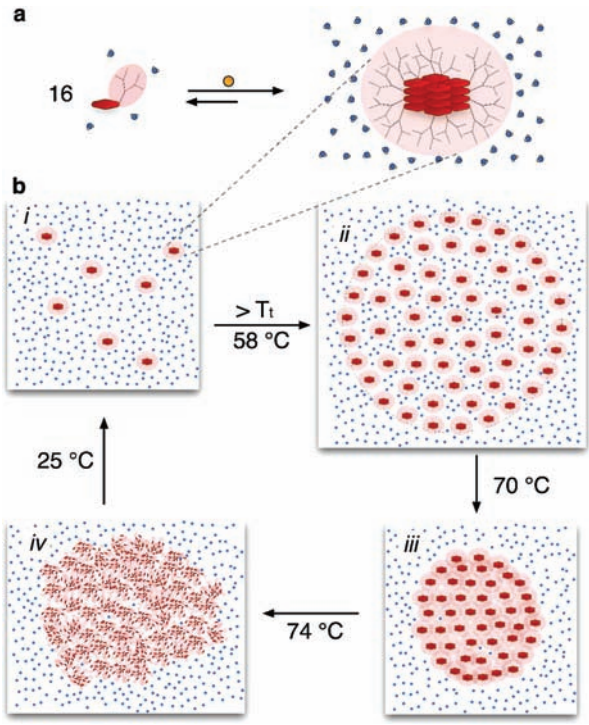

Figure 4. Proposed mechanism of hierarchical assembly. (a) Isothermal self-assembly of **2** to form $\mathbf{2}_{16}$. (b) Thermal induced assembly of $\mathbf{2}_{16}$. Upon reaching the T_t, $\mathbf{2}_{16}$ forms a hydrated globule (*ii*) with a hydrodynamic diameter of ~1 μm. (*iii*) The entropically favorable dehydration of the globule leads to a more compact nanoparticle with a diameter of ~325 nm. (*iv*) Beyond 74 °C the assemblies melt, inducing the formation of ill-defined aggregates of large polydispersity.

melting of the hexadecamers, which promotes the formation of larger polydisperse aggregates (Figure 4b,*iv*).

The results presented in this article provide compelling evidence that the self-assembly of nonpolymeric small molecules can lead to the development of smart, discrete, and well-defined supramolecules. Furthermore, reactions at the supramolecular level, in which two similar subunits with different hydrophobicities are mixed, enables the modulation of the LCST phenomenon. We are currently evaluating the scope of this strategy by synthesizing a series of derivatives of different hydrophobicities to fine-tune the T_t over a wider range. Studies aimed at exploring the possibility of using other stimuli, such as pH, to trigger the LCST phenomenon are underway. The extension of the LCST phenomenon from the macromolecular to the nonpolymeric supramolecular realm is likely to open the door to the development of novel smart materials for biomedical and nanotechnological applications.[1,4]

Acknowledgment. We thank NIH-SCoRE (Grant No. 2506GM08102) and NCRR-NIH (Grant No. P20 RR016470) for financial support. J.E.B. thanks the Alfred P. Sloan Foundation and NSF-IFN-EPSCoR (01A-0701525) for graduate fellowships. We also thank Adriana Herrera (UPRM) for help with DLS measurements; Dr. Maxime Guinel (UPRRP) for TEM images; and Amalia Ávila, Aura Collazo, and Luis Oquendo (UPRRP) for technical assistance during the initial stages of this project.

Supporting Information Available: Detailed synthetic procedures, characterization for all new compounds, experimental protocols, and NMR data. This material is available free of charge via the Internet at http://pubs.acs.org.

References

(1) (a) Yoshida, M.; Lahann, J. *ACS Nano* **2008**, *2*, 1101–1107. (b) Rodriguez-Hernandez, J.; Checot, F.; Gnanou, Y.; Lecommandoux, S. *Prog. Polym. Sci.* **2005**, *30*, 691–724. (c) de Las Heras Alarcon, C.; Pennadam, S.; Alexander, C. *Chem. Soc. Rev.* **2005**, *34*, 276–285.
(2) Simmons, D. S.; Sanchez, I. C. *Macromolecules* **2008**, *41*, 5885–5889.
(3) (a) Kumar, A.; Srivastava, A.; Galaev, I.; Mattiasson, B. *Prog. Polym. Sci.* **2007**, *32*, 1205–1237. (b) Chen, G.; Hoffman, A. S. *Nature* **1995**, *373*, 49–52.
(4) Dai, S.; Ravi, P.; Tam, K. C. *Soft Matter* **2009**, *5*, 2513–2533.
(5) Urry, D. *J. Phys. Chem. B* **1997**, *101*, 11007–11028.
(6) Schild, H. G. *Prog. Polym. Sci.* **1992**, *17*, 163–249.
(7) Gil, E. S.; Hudson, S. A. *Prog. Polym. Sci.* **2004**, *29*, 1173–1222.
(8) Urry, D. W.; Gowda, D. C.; Parker, T. M.; Luan, C. H.; Reid, M. C.; Harris, C. M.; Pattanaik; Harris, R. D. *Biopolymers* **1992**, *32*, 1243–1250.
(9) Chilkoti, A.; Dreher, M. R.; Meyer, D. E.; Raucher, D. *Adv. Drug Delivery Rev.* **2002**, *54*, 613–630.
(10) Lao, U.; Kostal, J.; Mulchandani, A.; Chen, W. *Nat. Protocols* **2007**, *2*, 1263–1268.
(11) Rzaev, Z.; Dinçer, S. *Prog. Polym. Sci.* **2007**, *32*, 534–595.
(12) Lehn, J. M. *Science* **2002**, *295*, 2400–2403.
(13) Whitesides, G. M. *Small* **2005**, *1*, 172–179.
(14) (a) Gubala, V.; Betancourt, J. E.; Rivera, J. M. *Org. Lett.* **2004**, *6*, 4735–4738. (b) Rivera-Sánchez, M. d. C.; Andújar-de-Sanctis, I.; Garía-Arriaga, M.; Gubala, V.; Hobley, G.; Rivera, J. M. *J. Am. Chem. Soc.* **2009**, *131*, 10403–10405. (c) Gubala, V.; De Jesus, D.; Rivera, J. M. *Tetrahedron Lett.* **2006**, *47*, 1413–1416. (d) Betancourt, J. E.; Martín-Hidalgo, M.; Gubala, V.; Rivera, J. M. *J. Am. Chem. Soc.* **2009**, *131*, 3186–3188.
(15) García-Arriaga, M.; Hobley, G.; Rivera, J. M. *J. Am. Chem. Soc.* **2008**, *130*, 10492–10493.
(16) Betancourt, J. E.; Rivera, J. M. *Org. Lett.* **2008**, *10*, 2287–2290.
(17) See Supporting Information.
(18) Schild, H. G.; Tirrell, D. A. *J. Phys. Chem.* **1990**, *17*, 163–249.
(19) Kisselev, A.; Manias, E. *Fluid Phase Equilib.* **2007**, *261*, 69–78.
(20) Urry, D. *Biopolymers* **1998**, *47*, 167–178.
(21) (a) Fernández-Trillo, F.; van Hest, J. C. M.; Thies, J. C.; Michon, T.; Weberskirch, R.; Cameron, N. R. *Chem. Commun.* **2008**, 2230–2232. (b) Yu, Y.; Nakamura, D.; DeBoyace, K.; Neisius, A. W.; McGown, L. B. *J. Phys. Chem. B* **2008**, *112*, 1130–1134.
(22) Schmitz, S.; Ritter, H. *Angew. Chem., Int. Ed.* **2005**, *44*, 5658–5661.
(23) Cohen, Y.; Avram, L.; Frish, L. *Angew. Chem., Int. Ed.* **2005**, *44*, 520–554.

JA9070927